Properties of the Intramolecular Excited Charge-Transfer States of Carbazol-9-yl Derivatives of Aromatic Ketones

Andrzej Kapturkiewicz*

Institute of Physical Chemistry, Polish Academy of Sciences, Kasprzaka 44/52, 01-224 Warsaw, Poland

Jacek Nowacki

Department of Chemistry, Warsaw University, Pasteura 1, 02-093 Warsaw, Poland

Received: March 17, 1999

Photoinduced intramolecular charge transfer (ICT) in a series of a newly synthesized N-bonded donor−acceptor derivatives of 3,6-di-*tert*-butylcarbazole containing benzophenone and acetophenone as an electron acceptor has been studied in solutions. In solvents more polar than butyl ether, excitation leads to an emissive singlet state. Solvatochromic effects on the spectral position and profile of the stationary fluorescence spectra clearly indicate the CT character of the emitting singlet states of all the compounds studied. An analysis of the CT fluorescence and absorption band shapes leads to the quantities relevant for the electron transfer in the Marcus inverted region. The analysis of the fluorescence rate constants (k_f) and corresponding transition dipole moments (M) indicate that Marcus theory can be applied for the quantitative description of the radiationless charge recombination processes in such cases, when an intersystem crossing to the excited triplet states may be neglected (i.e., in the polar solvent). This last reaction channel, however, seems to operate efficiently in nonpolar media in which charge-transfer fluorescence is totally quenched. The obtained results support the hypothesis that the photophysical behavior of a particular A−D compound can be predicted from the properties of its donor and acceptor moieties, taking also into account the manner of linking between the two subunits.

1. Introduction

An elucidation of the factors that influence the photophysical properties of the donor−acceptor compounds is important because the intramolecular excited-state electron transfer is a fundamental reaction playing a crucial role in a variety of photophysical, photochemical, and biochemical processes.[1,2] The relatively simple systems in which the photoinduced intramolecular electron transfer can take place are acceptor (A)−donor (D) subunits formally linked by a single bond. The electronic structure and conformation of the molecules in the excited charge transfer singlet states (^{1}CT) are the most important issues related to the photophysics of these compounds. The intrinsic factors controlling the excited-state electron transfer seem to be determined by the nature of the donor and the acceptor subunits, their relative orientation, as well as the reaction medium polarity.

Pursuing the analogy between CT optical spectroscopy and thermal electron transfer processes,[3−5] some information on the properties of these states can be independently obtained from the analysis of the charge transfer absorption $^1\text{CT} \leftarrow S_0$ and/or from the kinetics of the radiative and radiationless charge recombination $^1\text{CT} \rightarrow S_0$. Both processes are usually described using a "Golden rule" type formula leading to the appropriate rate constant that is dependent on two quantities: (i) a Franck−Condon weighted density of states, which contains the dependence of the rate on the energetic and nuclear parameters such as the free energy gap ΔG_{CT}, the outer-solvent (λ_s), and inner-intramolecular (λ_i) reorganization energies, the intramolecular nuclear−electronic coupling, and the frequencies ν_i of the vibronic states coupled to ET; (ii) the electronic matrix elements V_0 and V_1 describing the electronic coupling between the lowest excited charge transfer state ^{1}CT and the ground state S_0, or the locally excited states (with the electronic excitation localized on the donor or acceptor subunit) respectively. Relatively simple estimation of the above-mentioned parameters is possible from a band-shape analysis of the CT absorption[4,5] and/or fluorescence[5−13] and from the solvent polarity effects on the electronic transition dipole moments of the CT absorption (M_{abs}) and emission (M_{flu}),[7−11,13−25] correspondingly. Moreover, eventual solvent-induced changes of some of the above-mentioned quantities (e.g., electron transfer coupling elements or inner reorganization energies) allow also for the discussion of the structural changes occurring upon photoexcitation.

Our previously reported comparative investigations of the photophysics of relatively large aromatic donor−acceptor compounds[13,24,25] show a possibility to predict the photophysical behavior of a particular A−D system from the properties of its donor and acceptor subunits alone. One of the most important factors describing the properties of the given donor−acceptor pair is connected with the manner in which A and D subunits are bonded together and correspondingly with the interactions between the donor and acceptor subunits. It has been shown[13,24,25] that the respective electron transfer coupling elements (describing the electronic interactions between the CT state and the ground state and/or the locally excited states) are mainly determined by the interactions between the atoms forming the A−D bond. Their values can be theoretically predicted following the formalism proposed by Dogonadze et al.[26] from the data for the individual chromophores. A similar approach can be applied to describe the properties of the singlet ^{1}CT states (e.g., the transition dipole moments for the CT absorption $^1\text{CT} \leftarrow S_0$ and the fluorescence $^1\text{CT} \rightarrow S_0$) as well as the characteristics of the triplet ^{3}CT states[27] (e.g., the zero-field splitting parameters).

10.1021/jp990932t CCC: $18.00
Published on Web 09/24/1999

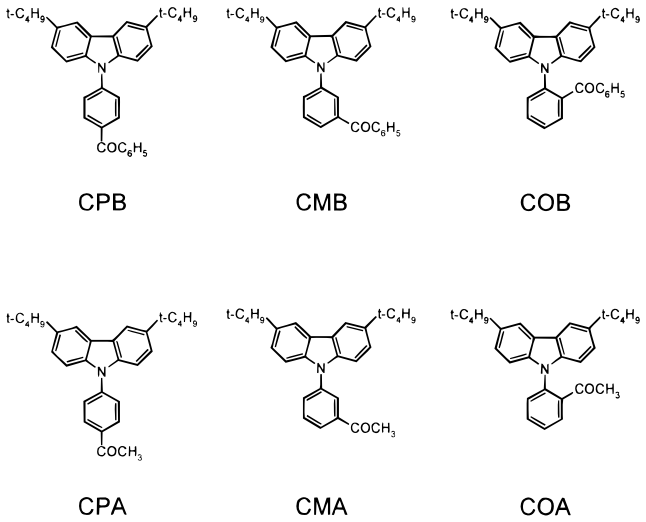

Figure 1. Formulas of electron donor−acceptor derivatives of 3,6-di-*tert*-butylcarbazole and their abbreviations used in the text.

This work is a part of our continuous studies done in order to better understand the properties of the intramolecular charge-transfer states and the mechanism of the radiative ($^1CT \leftarrow S_0$ and $^1CT \rightarrow S_0$) and nonradiative charge transfer transitions. The currently investigated carbazol-9-yl derivatives of selected aromatic ketones were chosen to test the application of the above-described simple model for the quantitative description of the fluorescent ^1CT states properties. The position of the carbonyl (acetyl or benzoyl) group with respect to the A−D bond in the given isomer was the main variable in our comparative investigations. The o, m, or p attachment of the acceptor group to 9-phenyl-3,6-di-*tert*-butylcarbazole leads to the different values of the LCAO coefficients on the carbon atom forming donor−acceptor bond and presumably to the differences in the electronic coupling matrix elements.

2. Experimental Section

2.1. Materials. The synthesis and purification of 3,6-di-*tert*-butylcarbazole (CAR) was performed by alkylation of carbazole with *tert*-butyl chloride and subsequent partial dealkylation.[28] Its electron donor−acceptor derivatives 4-(3,6-di-*tert*-butylcarbazol-9-yl)acetophenone (CPA), 3-(3,6-di-*tert*-butylcarbazol-9-yl)acetophenone (CMA), 2-(3,6-di-*tert*-butylcarbazol-9-yl)acetophenone (COA), 4-(3,6-di-*tert*-butylcarbazol-9-yl)benzophenone (CPB), 3-(3,6-di-*tert*-butylcarbazol-9-yl)benzophenone (CMB), and 2-(3,6-di-*tert*-butylcarbazol-9-yl)benzophenone (COB) were synthesized by means of the copper−bronze-catalyzed Ullmann condensation[29] of the corresponding bromoacetophenones (or bromobenzophenones) with 3,6-di-*tert*-butylcarbazole (Figure 1). The solvents used for absorption and emission studies, hexane (HEX), methylcyclohexane (MCH), butyl ether (BE), isopropyl ether (IPE), ethyl ether (EE), 1,2-dimethoxyethane (DME), butyl acetate (BA), ethyl acetate (EA), 1,2-dichloromethane (DCM), acetonitrile (ACN), *N*,*N*-dimethylformamide (DMF), *N*-methylpyrrolidone (NMP), dimethyl sulfoxide (DMSO), and 1-propanol (PrOH) were of spectroscopic or fluorescence grade (Aldrich and Merck). All solvents did not show any traces of luminescence and were selected to cover the wide range of the static dielectric permittivity values ϵ.[30]

2.2. Instrumentation and Procedures. Absorption spectra were recorded using a Shimadzu UV-2401 PC spectrometer. Emission and excitation spectra (corrected for the spectral sensitivity of the instrument) were measured by means of a FS 900 CDT fluorometer (Edinburgh Analytical Instruments). For the quantum yield (Φ_f) determinations, the solutions had identical optical densities at the excitation wavelength and were deaerated by saturation with preliminary purified and dried argon to avoid fluorescence quenching by oxygen. Quinine sulfate in 0.1 M H_2SO_4 (with $\Phi_f = 0.51$) served as the quantum yield standard.[31]

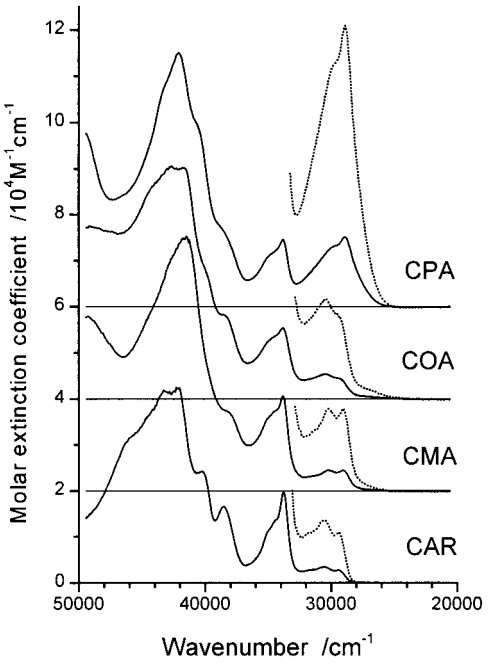

Figure 2. Room temperature absorption spectra recorded in acetonitrile for 3,6-di-*tert*-butylcarbazole (CAR) and its donor−acceptor derivatives containing acetophenone (CMA, COA, and CPA). Spectra of CMA, COA, and CPA are shifted along the *Y*-axis by a factor of 2×10^4. Low-energy parts of the absorption spectra are expanded by a factor of 4.

Fluorescence lifetimes were obtained using a FL 900 CDT time-resolved fluorometer (Edinburgh Analytical Instruments). The χ^2 test and the distribution of residuals were the main criteria in the evaluation of the quality of the fit of experimental decay curves. In all the cases studied the fluorescence decay was monoexponential on the nanosecond scale of observation.

The standard potentials of the one-electron oxidation E_{ox}(D) and reduction E_{red}(A) of all the compounds studied were determined by a cyclic voltammetry technique in the ACN and/or DMF solutions containing 0.1 M tetra-*n*-butylammonium tetrafluoroborate ($TBAPF_4$) as the supporting electrolyte. Measurements were carried out under argon on approximately 1 mM solutions. The analysis of the voltammograms, recorded at scan rate 100 mV/s, fast enough to minimize the influence of the radical ions' instabilities, allowed us to determine the standard redox potentials. The details of instrumentation used have been described previously.[32,33]

Semiempirical quantum chemical calculations have been performed using the AM1 method (from HYPERCHEM package developed by Hypercube Inc.). Other calculations (e.g., band-shape analysis of the CT fluorescence) were made by means of the least-squares method using a Sigma Plot package from Jandel Corp.

3. Results and Discussion

3.1. Absorption and Emission Spectra. Room temperature absorption spectra of the studied compounds are presented in Figures 2 and 3. The spectra show a superposition of the bands

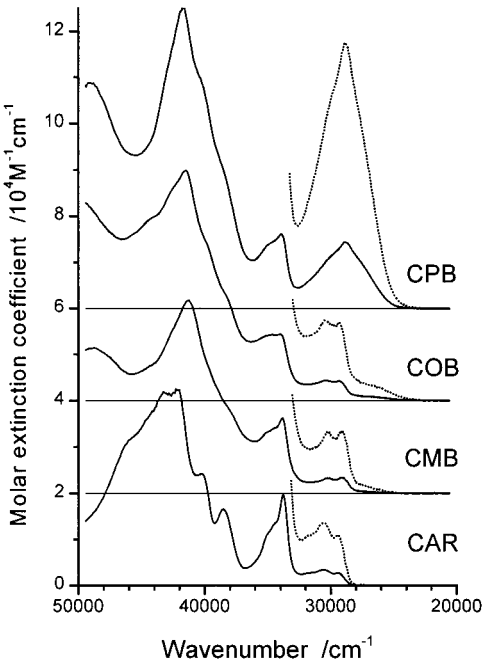

Figure 3. Room temperature absorption spectra recorded in acetonitrile for 3,6-di-*tert*-butylcarbazole (CAR) and its donor−acceptor derivatives containing benzophenone (CMB, COB and CPB). Spectra of CMB, COB, and CPB are shifted along the *Y*-axis by a factor of 2×10^4. Low-energy parts of the absorption spectra are expanded by a factor of 4.

corresponding to the donor and acceptor subunits, which seem to be only slightly perturbed by their interactions. Similarly to carbazole,[34,35] the first five absorption bands of CAR, being centered in *n*-hexane at 29 700, 33 800, 38 800, 40 200, and 43 100 cm^{-1}, were assigned to the final $^1(\pi,\pi^*)$ states of $^1A_1$, $^1B_2$, $^1B_2$, $^1A_1$, and $^1B_2$ symmetry, respectively. The two former bands correspond in Platt's notation to the ^1L_b and ^1L_a excited states, and the last one to the ^1B_a state. The transitions with a relatively high probability ($^1L_a \leftarrow S_0$ and $^1B_a \leftarrow S_0$) can be clearly observed in the absorption spectra of all the compounds studied. The effect of the lowest transitions in the acceptor moieties[36,37] is manifested by an increase of the width and intensity of the second and third absorption bands of the A−D molecules with respect to those of CAR. Detailed inspection of the low-energy absorption region of the studied A−D carbazole derivatives clearly indicates the presence of additional bands. Similarly, as was found for 3,6-di-*tert*-butylcarbazol-9-yl-dicyanobenzenes,[13] the separation of the low-energy CT absorption band is due to the increasing electron affinity of the acceptor (ketone) subunit and the corresponding lowering of the CT state energy. The red shift of the lowest absorption band for benzophenone derivatives as compared to acetophenone analogs may be simply related to the electron affinities of the given acceptor subunits. The attribution of the lowest absorption bands to a $^1CT \leftarrow S_0$ transition is additionally supported by the comparison of the reduced absorption bands (as plotted in the form $\epsilon(\tilde{\nu}_a)/\tilde{\nu}_a$ vs $\tilde{\nu}_a$) and the emission profiles (i.e., a plot of the normalized reduced intensity $I(\tilde{\nu}_f)/\tilde{\nu}_f^3$ vs $\tilde{\nu}_f$). The corresponding spectra seem to exhibit a mirror relationship. Figure 4 shows the corresponding spectra for COB in ACN solution as the representative example. An intrinsic increase of the first absorption band intensity for CPB and CPA molecules (as compared to the other isomers studied) indicates that two transitions $^1CT \leftarrow S_0$ and $^1(\pi,\pi^*) \leftarrow S_0$ are superimposed in this band.

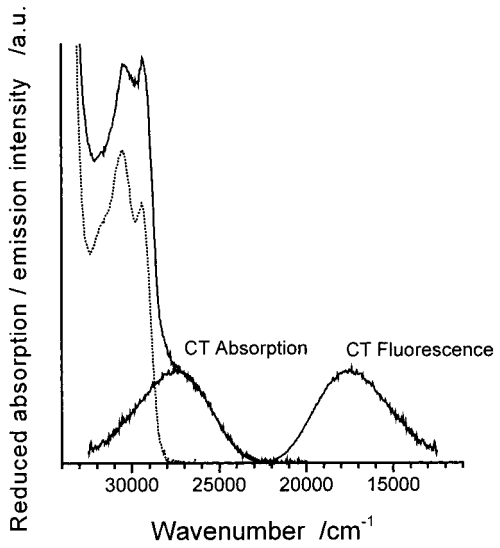

Figure 4. Room temperature reduced and normalized absorption and fluorescence spectra (see text) for COB in acetonitrile. The lowest CT absorption band is separated under the assumption that the reduced CT absorption and fluorescence spectra exhibit a mirror relationship. Dotted line (resulting from a subtraction of the lowest CT absorption from the total absorption) corresponds to excitation localized in the 3,6-di-*tert*-butylcarbazole (CAR) moiety.

Carbazol-9-yl derivatives of the aromatic ketones, similarly as other large aromatic A−D molecules, exhibit a single fluorescence band at room temperature. A considerable red shift of the fluorescence spectral position (and the increase of the Stokes shift and of the emission bandwidth) with increasing solvent polarity point clearly to the polar character of the fluorescent states. This finding, together with the UV−VIS absorption data, clearly indicates that the absolute values of the excited state dipole moments $|\vec{\mu}_e|$ are much higher than those of the ground state $|\vec{\mu}_g|$. It should be noted that in contrast to most of the large A−D aromatic compounds, no (or only trace) emission is observed in nonpolar (MCH or HEX) or weakly polar (BE) solvents. The emissive properties of the studied A−D systems are enhanced in polar media. The fluorescence intensity initially increases with the solvent polarity (starting from IPE), maximizes for the moderately polar solvents (e.g., for both para isomers, CPA and CPB, the observed quantum yield Φ_f approaches the values close to unity in EA or DME), and decreases thereafter in more polar solvent (such as ACN or DMF). This behavior is most probably connected with the presence of two competitive nonradiative excited state deactivation channels—the intersystem crossing to the triplet manifold and a direct radiationless charge recombination process in the singlet manifold.

The low-temperature emission spectra of acetophenone as well as benzophenone derivatives were recorded at 77 K in glassy solvents such as MCH or PrOH. In both rigid matrices, all of the compounds studied emit mainly very intense phosphorescence and similarly as at room temperatures in nonpolar environment only a very weak (if any) fluorescence. The observed spectra are presented in Figures 5 and 6. The molecules containing acetophenone as an electron acceptor show structured phosphorescence spectra with the vibrational structure and the spectral positions of the 0,0 band similar to those observed for CAR (the carbazole T_1 state is of ^3L_a type[38]). These results indicate the dominant $^3(\pi,\pi^*)$ character of the phosphorescent triplet states with the excitation being mainly localized in the carbazole moiety. On the contrary, the phosphorescence spectra of the benzophenone derivatives correspond to the $^3(n,\pi^*)$ state[38]

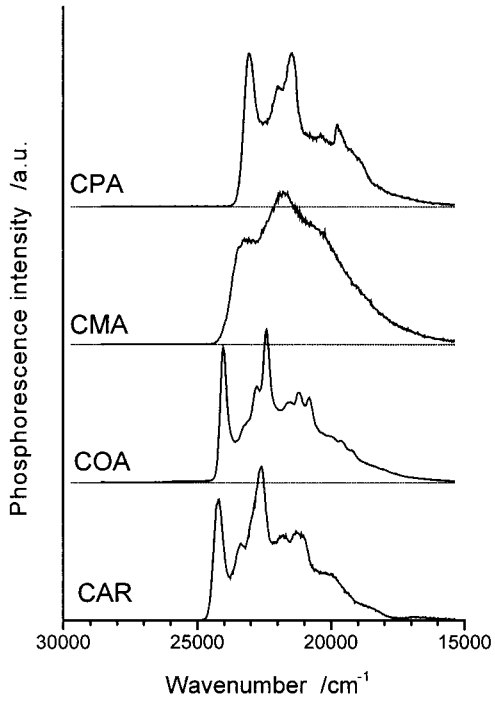

Figure 5. Phosphorescence spectra (in 1-propanol glass at 77 K) of 3,8-di-*tert*-butylcarbazole (CAR) and its donor−acceptor derivatives (CMA, COA, and CPA) containing acetophenone as an acceptor subunits.

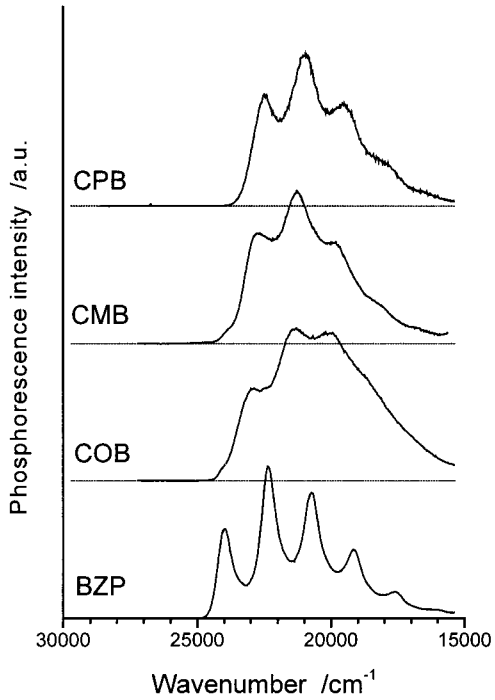

Figure 6. Phosphorescence spectra (in 1-propanol glass at 77 K) of benzophenone (BZP) and its donor−acceptor derivatives (CMB, COB, and CPB) containing 3,8-di-*tert*-butylcarbazole as a donor subunit.

localized in the acceptor subunit (the energy of the benzophenone T_1 state, contrary to acetophenone, is somewhat lower than that of carbazole[39]). The observed changes of the shape and spectral position of phosphorescence (as compared to the reference systems) can be probably attributed to the interactions between locally excited triplet T_1 and ^{3}CT state. The postulated nature of the lowest emissive triplet state agrees well with the preliminary results of the phosphorescence lifetime τ_{pho} measurements.

TABLE 1: Spectral Position of the Fluorescence Maxima ($\tilde{\nu}_f$), Quantum Yields (Φ_f), Decay Times (τ_{flu}), and Resulting Radiationless (k_{nr}) and Radiative (k_f) Rate Constants, and Electronic Transition Dipole Moments (M) of the Carbazol-9-yl Derivatives of Aromatic Ketones in *N,N*-Dimethylformamide Solutions at Room Temperature

substance	$\tilde{\nu}_f{}^a$ (cm^{-1})	$\Phi_f{}^b$	$\tau_{flu}{}^b$ (ns)	k_{nr} (s^{-1})	k_f (s^{-1})	M (D)
CPB	18 400	0.29	9.8	7.2×10^7	3.0×10^7	2.3
COB	19 000	0.058	10.5	9.0×10^7	5.5×10^6	0.9
CMB	18 000	0.053	20.4	4.6×10^7	2.6×10^6	0.7
CPA	19 400	0.27	10.5	7.0×10^7	2.6×10^7	2.0
COA	20 075	0.091	16.7	5.5×10^7	5.5×10^6	0.85
CMA	19 550	0.071	22.6	4.1×10^7	3.1×10^6	0.7

[a] Scatter of results is ±100−150 cm^{-1}. [b] Error is about 10%. Thus, the maximal error is about 20% for the rate constants k_f and k_{nr} and about 10% for the transition moment M.

The spectroscopic properties of the A−D system studied in the present work are in accordance with the previously reported data for the carbazol-9-yl derivatives of aromatic nitriles.[13,27] The main difference (lack of the fluorescence in nonpolar media) arises most probably from the nature of the lowest acceptor triplet state with $^3(n,\pi^*)$ nature and is connected with the spin−orbit coupling effects.

3.2. Excited State Dipole Moments. The lowest CT absorption bands of the studied carbazole derivatives show a small red shift with increasing solvent polarity in agreement with the theory of dielectric polarization.[40] Such behavior of the absorption band is expected for the transitions from a state with a small dipole moment to a state with a larger one (eq 1). Assuming a point dipole situated in the centre of the spherical cavity and neglecting the mean solute polarizability α in the states involved in the transition ($\alpha \cong \alpha_e \cong \alpha_g = 0$), the solvatochromic effects on the spectral position of the CT absorption spectra can be given by[41−44]

$$hc\tilde{\nu}_{abs} \cong hc\tilde{\nu}_{abs}(\mathrm{vac}) - \frac{2\vec{\mu}_g(\vec{\mu}_e - \vec{\mu}_g)}{a_o{}^3}\left[\frac{\epsilon - 1}{2\epsilon + 1} - \frac{1}{2}\frac{n^2 - 1}{2n^2 + 1}\right] \quad (1)$$

where $\tilde{\nu}_{abs}$ and $\tilde{\nu}_{abs}(vac)$ are the spectral positions of the absorption maxima and the value extrapolated to the gas phase, respectively. The quantities $\vec{\mu}_g$ and $\vec{\mu}_e$ are the dipole moments of the solute in the ground and excited state, a_o is the effective radius of the Onsager cavity,[45] ϵ and n are the static dielectric constant and the refractive index of the solvent, respectively.

Under the same assumptions as used for eq 1, the following expression may be applied for the description of the solvent induced changes of the fluorescence maxima

$$hc\tilde{\nu}_{flu} \cong hc\tilde{\nu}_{flu}(\mathrm{vac}) - \frac{2\vec{\mu}_e(\vec{\mu}_e - \vec{\mu}_g)}{a_o{}^3}\left[\frac{\epsilon - 1}{2\epsilon + 1} - \frac{1}{2}\frac{n^2 - 1}{2n^2 + 1}\right] \quad (2)$$

where $\tilde{\nu}_{flu}$ and $\tilde{\nu}_{flu}(vac)$ are the spectral positions of the solvent-equilibrated fluorescence maxima and the value extrapolated to the gas phase, respectively. The excited-state dipole moments $\vec{\mu}_e$ can be estimated by the fluorescence solvatochromic shift method[41−44] due to the fact that, in our case, the excited states live sufficiently long with respect to the orientational relaxation time of the solvent (cf. Table 1). The compounds studied show a satisfying linear correlation between the energy $hc\tilde{\nu}_{flu}$ and the Lippert−Mataga solvent polarity function (Figure 7). The obtained fluorescence data allow to determine the $\vec{\mu}_e$ ($\vec{\mu}_e - \vec{\mu}_g$)/$a_o{}^3$ values (collected in the Table 2) and, correspondingly

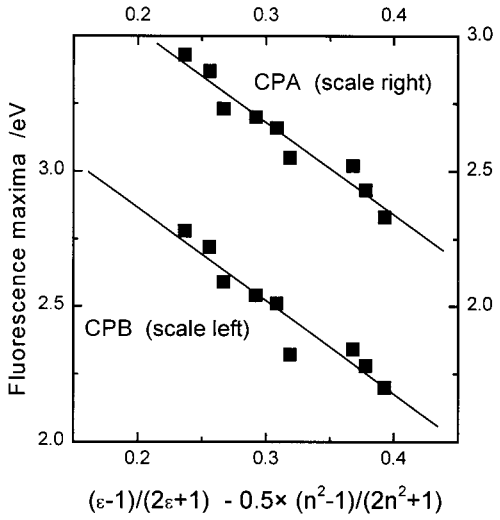

Figure 7. Solvatochromic shift of the energy related to the CT fluorescence maxima for CPB and CPA as a function of the solvent polarity (according to eq 2).

TABLE 2: Slopes of the Solvatochromic Plots of the CT Fluorescence and Results from the CT Band-Shape Analysis of the A−D Carbazole Derivatives

substance	$\vec{\mu}_e(\vec{\mu}_e - \vec{\mu}_g)/a_o^3$ (eV)	$(\vec{\mu}_e^2 - \vec{\mu}_g^2)/a_o^3$ (eV)	$(\vec{\mu}_e - \vec{\mu}_g)^2/a_o^3$ (eV)	λ_i (eV)	$h\nu_i$ (eV)	$\delta\lambda_o$ (eV)
CPB	1.70	1.53	1.98	0.26	0.19	0.10
COB	1.06	1.35	0.99	0.28	0.20	0.10
CMB	1.48	≈1.25	*a*	0.30	0.19	
CPA	1.70	1.50	2.05	0.27	0.20	0.06
COA	1.30	1.44	1.14	0.30	0.20	0.10
CMA	1.40	≈1.14	*a*	0.31	0.19	

[a] The corresponding plots exhibit the deviations from linearity, see text.

(considering the limitations of the model), to estimate of the excited state dipole moments $\vec{\mu}_e$. It was done under the assumption that $|\vec{\mu}_e| \gg |\vec{\mu}_g|$ and with the effective spherical radius of the A−D molecules $a_o \approx 0.6$ nm (as estimated from the molecular dimensions of the compounds calculated by molecular mechanics). The obtained values of μ_e are in the range of 15−20 D and 20−25 D for the molecules with and without carbonyl group in the ortho position with respect to the A−D bond, respectively. Such large values correspond to a CT distance of about 0.40−0.45 nm, which roughly agrees with the center-to-center distance between the donor and acceptor moieties of the compounds. It suggests that the full (or nearly full) electron transfer takes place in all of the A−D systems studied.

This conclusion is in excellent agreement with a linear relationship found between the CT fluorescence energies and the differences in the redox potentials corresponding to the oxidation of the donor subunit $E_{ox}(D)$ and the reduction of the acceptor moiety $E_{red}(A)$ in the A−D molecules. The correlation for the studied A−D compounds is shown in Figure 8 together with the results reported previously[13] for carbazol-9-yl derivatives of aromatic nitriles. In the above correlation the values of $E_{ox}(D) - E_{red}(A)$ are determined from the cyclic voltametry data obtained for the given A−D molecule in ACN and/or DMF containing 0.1 M $TBABF_4$ (an exemplary voltammogram is shown in Figure 9). The obtained values are very similar to those expected from the electrochemical properties of the donor and acceptor alone; the standard oxidation potentials $E_{ox}(D)$ as well as the standard reduction potentials $E_{red}(A)$ were found close to the values found for CAR[46] and a proper ketone,[47]

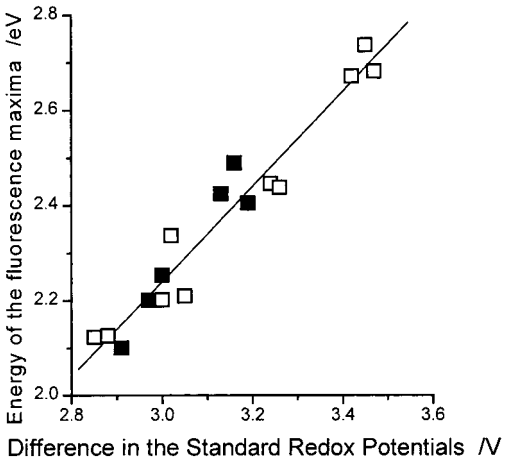

Figure 8. Correlation between the energy of the fluorescence maxima of the carbazo-9-yl A−D derivatives of ketones (solid squares) and nitriles (open squares) and the difference in the standard redox potentials (acetonitrile or *N*,*N*-dimethylformamide solutions at room temperature). Solid line corresponds to the "theoretical" slope of 1.00.

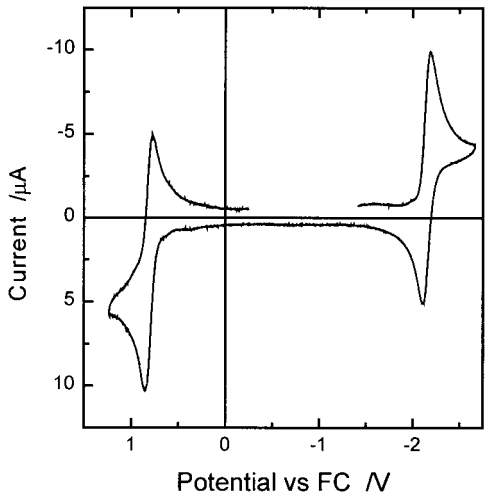

Figure 9. Room temperature cyclic voltammogram of 1 mM CPB in 0.1 M $TBABF_4$/ACN solutions. (Pt working electrode; scan rate = 100 mV/s, potential scale according to ferrocene/ferricene internal reference redox system).

respectively. The small shift of $E_{red}(A)$ to more negative potentials can be explained by the electron-donating properties of 3,6-di-*tert*-butylcarbazole bonded to the acceptor subunit. Correspondingly, the small shift of $E_{ox}(D)$ to more positive potentials arises from the electron-withdrawing character of the acceptor moiety. The $E_{red}(A)$ and $E_{ox}(D)$ values indicate also (in agreement with the absorption spectra) that both subunits of all the A−D molecules studied interact very weakly.

3.3. CT Band-Shape Analysis. Additional information on the properties of the excited CT states can be obtained from the analysis of the charge transfer absorption ($^1CT \leftarrow S_0$) and/or the radiative charge recombination ($^1CT \rightarrow S_0$). As has been shown by Marcus, Hush, and Ulstrup, the following expression for the molar absorption coefficient $\epsilon(\tilde{\nu}_a)$ for CT absorption of a given photon with energy $hc\tilde{\nu}_a$ can be derived[3,4]

$$\frac{\epsilon(\tilde{\nu}_a)}{n\tilde{\nu}_a} = \frac{8\pi^3}{3\ln 10}\frac{M^2}{c}\sum_{j=0}\frac{e^{-s}S^j}{j!}\sqrt{\frac{1}{4\pi\lambda_o k_B T}} \exp\left[-\frac{(\Delta G_{CT} + \lambda_o + jh\nu_i - hc\tilde{\nu}_a)^2}{4\lambda_o k_B T}\right] \quad (3)$$

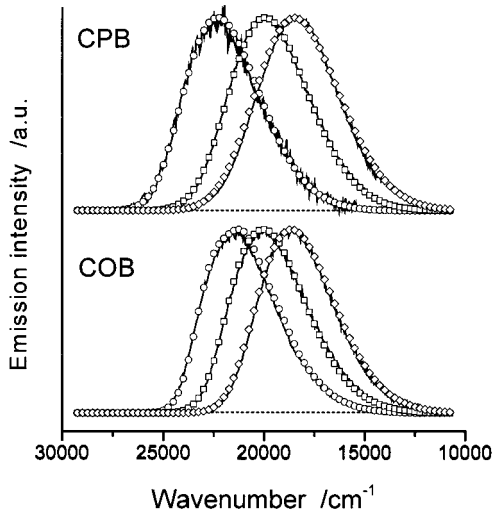

Figure 10. Room temperature CT fluorescence spectra of CPB and COB in isopropyl ether, dimethoxyethane, and *N*,*N*-dimethylformamide (from left to right, respectively) and the corresponding numerical fit (circles, squares, and diamonds, correspondingly) according to eq 4.

where M is the electronic transition dipole moment, k_B the Boltzmann constant, c the velocity of light, and T temperature. In a similar way, the CT fluorescence profile, i.e., the rate $I(\tilde{\nu}_f)$ of the emission of a given photon with energy $hc\tilde{\nu}_f$, is given by

$$\frac{I(\tilde{\nu}_f)}{n^3\tilde{\nu}_f^3} = \frac{64\pi^4}{3h} M^2 \sum_{j=0} \frac{e^{-s}S^j}{j!} \sqrt{\frac{1}{4\pi\lambda_o k_B T}} \exp\left[-\frac{(\Delta G_{CT} + \lambda_o + jh\nu_i + hc\tilde{\nu}_f)^2}{4\lambda_o k_B T}\right] \quad (4)$$

The electron−vibration coupling constant S is equal to the inner reorganization energy λ_i expressed in units of vibrational quanta ($S = \lambda_i/h\nu_i$). The inner reorganization energy λ_i corresponds to the high-frequency motions (represented by a single "averaged" mode characterized by ν_i) associated with the changes in the solute bond lengths and angles. The reorganization energy λ_o is related to the low-frequency motions such as reorientation of the solvent shell (λ_s) as well as any other low- and medium-frequency nuclear motions of the solute ($\delta\lambda_o$) undergoing electron transfer.

Following the procedure of the band-shape analysis of the CT fluorescence spectra proposed by Cortes, Heitele, and Jortner,[12] the quantities relevant for the electron transfer (i.e., ΔG_{CT}, $h\nu_i$, λ_i, and λ_o) were varied as free fit parameters. It has been done with an assumption that the electronic transition dipole moment value M is independent of the emitted (absorbed) photon energy. It should be stressed that nearly the same results are obtained in the analysis taking into account the dependence of M vs $\tilde{\nu}_f$ (cf. also ref 12). Representative examples of the numerical fits (within a single high-frequency mode approximation according to eq 4) of the CT fluorescence spectra are presented in Figure 10; the experimental emission profiles of all the A−D compounds studied in the whole range of the solvents could be adequately reproduced. It should be noted, however, that ΔG_{CT} and λ_o as well as $h\nu_i$ and λ_i turn out to be somewhat correlated, leading to a numerical uncertainty (standard deviations) of their values of about ±0.02 eV. Because of the model approximations, however, the real uncertainty can be somewhat larger. The mirror relationship between the reduced CT absorption bands (as plotted in the form $\epsilon(\tilde{\nu}_a)/\tilde{\nu}_a$ vs $\tilde{\nu}_a$) and the CT emission spectra (i.e., a plot of the normalized reduced intensity $I(\tilde{\nu}_f)/\tilde{\nu}_f^3$ vs $\tilde{\nu}_f$) is observed in the case of the system studied (cf. Figure 4). Consequently, the CT absorption and CT fluorescence bands are reproducible with the same set of the energetic and nuclear parameters.

TABLE 3: Free Energies of the Excited ^{1}CT States of the Carbazol-9-yl Derivatives of the Aromatic Ketones in Acetonitrile and *N*,*N*-Dimethylformamide Solutions. Comparison between the Values Obtained from the Electrochemical and Spectroscopic Investigations

	acetonitrile			*N*,*N*-dimethylformamide		
substance	$F(E^\circ_{ox} - E^\circ_{red})^a$	$-\Delta G_{CT}{}^b$	$-w_R$	$F(E^\circ_{ox} - E^\circ_{red})^a$	$-\Delta G_{CT}{}^b$	$-w_R$
CPA				3.19	3.16	0.03
CMA				3.13	3.13	0.00
COA				3.16	3.02	0.14
CPB	2.97	2.97	0.00	3.07	3.09	−0.02
CMB	2.91	2.84	0.07	2.91	2.95	−0.04
COB	3.00	2.79	0.21	3.04	2.81	0.25

[a] Scatter of the results is ±0.02 eV. [b] The estimated uncertainty of the computed values (band-shape analysis) is ca. 0.02 eV. Thus, the maximal error is about 0.04 eV for the w_R term.

The values of ΔG_{CT} and λ_o extracted from the band-shape analysis depend on the solvent polarity, as expected. The more polar is the medium, the larger is the outer reorganization energy (λ_o) and the smaller is the energy gap between the ground and excited ^{1}CT states (ΔG_{CT}), in agreement with the dielectric continuum model of solvation. An analysis of the solvent effects on ΔG_{CT} is possible according to eq 5 (based on the Onsager theory[45] of the dipole solvation energy):

$$\Delta G_{CT} = \Delta G_{CT}(\text{vac}) + \frac{\vec{\mu}_e{}^2 - \vec{\mu}_g{}^2}{a_o{}^3}\left[\frac{\epsilon - 1}{2\epsilon + 1}\right] \quad (5)$$

The experimental values of $(\vec{\mu}_e{}^2 - \vec{\mu}_g{}^2)/a_o{}^3$ term are collected in Table 2. These values are similar to those obtained from the solvatochromic data ($\vec{\mu}_e(\vec{\mu}_e - \vec{\mu}_g)/a_o{}^3$ parameters). Both values for the given A−D system should be identical within the dielectric continuum approximation, if the ground state dipole moment is equal zero. This is not the case with the studied A−D compounds which have the ground state dipole moments in the range of 2−4 D (from AM1 calculations). Moreover, for both meta derivatives (contrary to ortho and para isomers) some deviations from the linear fit (ΔG_{CT} vs $(\epsilon - 1)/(2\epsilon + 1)$) are observed. The effect is small and similarly to λ_o (as discussed below) most probably arises from the solvent induced changes in the excited CT state dipole moments.

It should be emphasized that the values of ΔG_{CT} obtained from the spectroscopic data agree very well with the independent estimations of the energy levels of the ^{1}CT states based on the electrochemical measurements.[49,50] It may be done according to eq 6 in which the last term corresponds to the Coulombic stabilization energy (between the elementary charges e_o at the separation distance r_{AD}) in the radical ion pair (as forming a CT state)

$$\Delta G_{CT} \cong F(E_{red}(A) - E_{ox}(D)) - w_R = F(E_{red}(A) - E_{ox}(D)) - \frac{e_o{}^2}{\epsilon r_{AD}} \quad (6)$$

Table 3 presents the results of such comparison in DMF and ACN solutions. The respective values of coulombic attraction terms w_R are very small for meta and para isomers and

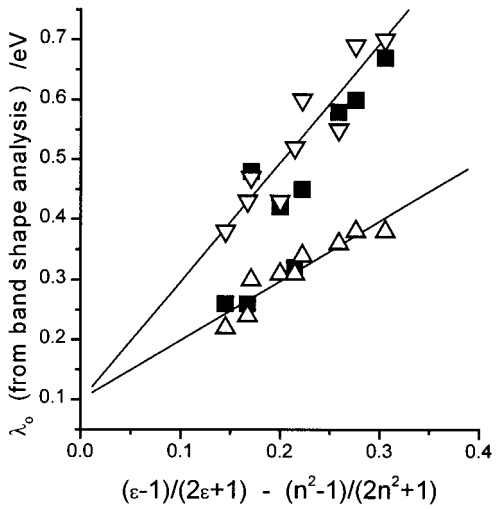

Figure 11. Correlation between the reorganization energy λ_o and the solvent polarity function (according to eq 7) for *N*-carbazolyl derivatives of benzophenone: (▽) CPB, (△) COB, and (■) CMB.

somewhat larger for ortho systems. It corresponds very well to the different distances between redox centers and agrees also with the experimental values of the excited state dipole moments.

The quantitative discussion of λ_o, values is possible according to eq 7, which is somewhat different from the classical Marcus expression but more suitable for the direct comparison with the results of the solvatochromic investigations[23,48]

$$\lambda_o = \delta\lambda_o + \lambda_s = \delta\lambda_o + \frac{(\vec{\mu}_e - \vec{\mu}_g)^2}{a_o^3}\left[\frac{\epsilon - 1}{2\epsilon + 1} - \frac{n^2 - 1}{2n^2 + 1}\right] \quad (7)$$

The dependence of the reorganization energy λ_o on the solvent polarity function is presented in Figure 11 for the A−D systems containing the benzophenone subunit. Nearly the same picture was obtained also for the case of acetophenone derivatives. For both ortho and para isomers the values of $(\vec{\mu}_e - \vec{\mu}_g)^2/a_o^3$ obtained from the slopes of the plots corresponding to eq 7 agree with those obtained from the other solvatochromic data (cf. Table 2). The meta isomers, however, show somewhat different behavior. Linearization of the experimental λ_o values is not possible without the physically meaningless assumption of the negative intercepts $\delta\lambda_o$. The observed inconsistency arises probably from the solvent-induced changes of the solute geometry (i.e., conformation) of the excited CT state approximated as the contact ion pair. In low-polarity solvents (with $\epsilon < 5$), Coulombic attraction between oppositely charged carbonyl group (in acceptor subunits) and positively charged nitrogen atom (in donor subunit) leads to conformation which corresponds to the lower value of the excited state dipole moment. In more polar solvent (with $\epsilon > 5$), Coulombic attraction forces are smaller and the effects caused by an increase of the excited state solvation energy prevail, leading to the conformation with a higher value of the excited state dipole moment. From sterical reasons such conformation changes are only possible for the meta isomers (cf. Figure 12). The values of $\delta\lambda_o$ estimated from the intercepts of the plot of λ_o vs solvent polarity function (eq 5) are in the range of 0.08−0.10 eV for all the A−D carbazole derivatives. As mentioned above, $\delta\lambda_o$ is probably connected with the low-frequency intramolecular vibration mode ($\tilde{\nu}_L < 200$ cm^{-1}, e.g. associated with librations, internal rotations) and/or with the medium-frequency mode of the solute ($\tilde{\nu}_M \cong 300-600$ cm^{-1}, e.g., an aromatic ring skeletal vibration).

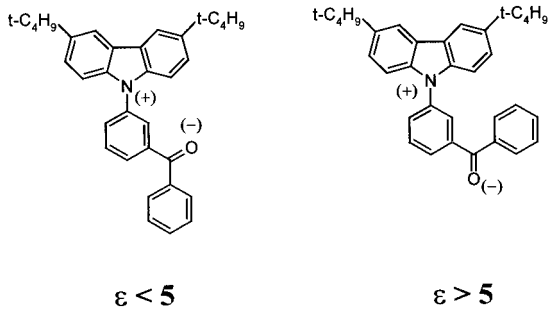

ε < 5 **ε > 5**

Figure 12. Two possible conformers of the excited ^{1}CT states of carbazol-9-yl derivatives of benzophenone in low polar ($\epsilon < 5$) and high polar ($\epsilon > 5$) media, respectively.

For the given A−D molecule, the quantities λ_i and $h\nu_i$ (collected in Table 2) have been found to be nearly constant (with uncertainty of about ±0.02 eV) over the whole solvents range. The $h\nu_i$ values (being about 0.19−0.20 eV) seem to correspond to the stretching vibrations of the C−C and C−N bonds.[51] The experimental values of λ_i are in a reasonable agreement with the results of AM1 semiempirical calculations. The difference between the computed values of the heat of formation of the donor in its equilibrium nuclear geometry and in the conformation corresponding to the equilibrium geometry of its radical cation is added to the respective value calculated for the acceptor and its radical anion. The sum of these energy differences can be regarded as a lower limit of the inner reorganization energies. The above approach neglects, however, the contribution related to the changes of the nitrogen−carbon bond between the donor and acceptor subunits. The calculated values (being in the range of 0.25−0.27 eV) agree very well with those obtained experimentally (Table 2).

An independent verification of the computed parameters ΔG_{CT}, λ_i, and λ_o is possible due to the following approximate expressions for the maxima of the reduced CT absorption and fluorescence spectra[5−13]

$$^1/_2(hc\tilde{\nu}_{abs} - hc\tilde{\nu}_{flu}) \cong \lambda_o + \lambda_i \quad (8)$$

$$^1/_2(hc\tilde{\nu}_{abs} + hc\tilde{\nu}_{flu}) \cong -\Delta G_{CT} \quad (9)$$

The experimental positions of the maxima of the reduced CT absorption and CT fluorescence spectra as well as the energy of the corresponding Stokes shift agree well with those predicted by the band-shape analysis (within the accuracy of the fitting procedure (ca. 3 × 0.02 eV)). It indicates that the dielectric continuum model describes quite well the observed solvent effects in our particular case of the large π-aromatic A−D systems.

The absence of the solvent-induced changes in λ_i together with small values of $\delta\lambda_o$ indicates also the lack of any significant intramolecular nuclear motions (e.g. rotations around A−D bond) upon excitation for the studied A−D systems with carbonyl group in ortho or para position. Especially, the twist angle between the donor and acceptor moieties in the emitting ^{1}CT state seems to be similar to that in the ground state. The conclusion appears to be also fulfilled for the meta isomers where two conformers seem to have the same energies, with only somewhat restricted internal rotation of carbonyl group.

3.4. Radiative Rate Constants and Electron Transfer Coupling Elements. If we apply a simple kinetic model of an irreversible excited charge transfer state formation (with 100% efficiency), the radiationless (k_{nr}) and radiative (k_f) rate constants can be determined from the CT fluorescence quantum yields

Φ_f and lifetimes τ_{flu}

$$k_f = \Phi_f/\tau_{flu} \tag{10}$$

$$k_{nr} = (1 - \Phi_f)/\tau_{flu} \tag{11}$$

The experimental k_f and k_{nr} values for all the A−D carbazole derivatives in DMF solutions are collected in Table 1 together with the corresponding values of electronic transition dipole moments M calculated according to[52]

$$k_f = \frac{64\pi^4}{3h} n^3 \tilde{\nu}_{flu}{}^3 |M|^2 \tag{12}$$

The important result is that the values of M for emission processes are comparable with those estimated for the corresponding absorption (estimated from the CT band intensity). This finding (in agreement with the conclusion from the CT band-shape analysis) supports the lack of any significant conformational changes (especially connected with the angle between the planes of the donor and acceptor subunits) accompanying the excited state charge separation. Consequently, the observed values of the transition dipole moment (for CT absorption as well as emission) can be interpreted in the same way.

Generally, the electronic transition dipole moments are discussed[19] in terms of the electronic coupling between the ^{1}CT and S_0 states (Mulliken's two-state model[53]) and/or between the ^{1}CT state and close lying ^{1}LE state of the appropriate symmetry (intensity "borrowing" mechanism as advanced by Murrell[54]). In the case of fluorescence the following expression[19] can be applied for the estimation of the appropriate contributions:

$$M = \frac{V_0(\vec{\mu}_e - \vec{\mu}_g)}{hc\tilde{\nu}_{flu}} + \sum_i \frac{V_i M_i}{E_i - hc\tilde{\nu}_{flu}} \tag{13}$$

where V_0 and V_i are the electronic coupling elements between the ^{1}CT state and the ground state or between the ^{1}CT state and ^{1}LE states "i" of energy E_i, respectively; M_i is the electronic transition moment corresponding to the radiative transition ^{1}LE $\rightarrow S_0$. Similarly as was found for carbazol-9-yl derivatives of aromatic nitriles,[13] the first term in eq 13 seems to be mostly responsible for the observed M values for the A−D molecules studied. The analysis of the absorption spectra (cf. Figures 2 and 3) shows no spectral evidence of significant role of the mechanism expressed by the second term in eq 18. For example, the increase of the intensity of the first absorption band in CPB and CPA with respect to that of CAR does not introduce any marked decrease of the intensity of the bands corresponding to the donor and acceptor subunits.

The values of the electronic coupling element V_0 (as estimated from the experimental M values under the assumption that the first term in eq 13 plays a dominant role) are found to be correlated with the position of the carbonyl (acetyl or benzoyl) group with respect to the A−D bond. Such behavior seems to be understandable within the concept that the electronic coupling elements are mainly determined by the interactions between the atoms forming the A−D bond. The formalism proposed by Dogonadze et al.[26] and adapted for the intramolecular charge-transfer in refs 13, 24, and 25 allows a quantitative description of this finding. The electronic coupling element V_0 responsible for such kind of interactions can be estimated according to eq 14:

$$V_0 \cong C^A_{LUMO}\, C^D_{HOMO}\, \beta_{AD} \cos(\Theta_{AD}) + \text{const} \tag{14}$$

where Θ_{AD} is the angle between the planes of the donor and acceptor subunits, and C^A_{LUMO} and C^D_{HOMO} are the corresponding LCAO coefficients of the $2p_z$ atomic orbitals (where z is the axis perpendicular to the acceptor or donor ring) of the carbon and nitrogen atoms forming A−D bond, respectively. The quantity const is related to the electronic interactions between the remaining pairs of atoms in a given A−D molecule (this contribution is relatively small and negligible). The values C^A_{LUMO} and C^D_{HOMO} may be obtained in two independent ways: (i) from semiempirical AM1 calculations and (ii) from the hyperfine structure of the ESR spectra[55] of the respective radical cation[56] and anion.[57,58] Both methods yield very similar values. Assuming the resonance integral $\beta_{AD} = 1.8$ eV (carbon−nitrogen bond) and neglecting the electronic interactions between the remaining pairs of atoms in the donor−acceptor systems (i.e., const = 0) the value of V_0 has been calculated from eq 14. It was done using the necessary values of Θ_{AD} angle obtained by means of AM1 calculations (crystallographic data are available only for *N*-pyridyl and *N*-phenylcarbazoles[59]). The calculated V_0 values agree quite well with those found experimentally; the corresponding correlation is presented in Figure 13 (for comparison also the data for other A−D systems[13,25] are included).

Similarly, the electronic coupling elements V_i between the ^{1}CT state and ^{1}LE states (either connected with the donor $V_1{}^D$ or with acceptor $V_1{}^A$ can be described:

$$V_1{}^A \cong C^A_{HOMO}\, C^D_{HOMO}\, \beta_{AD} \cos(\Theta_{AD}) + \text{const} \tag{15}$$

$$V_1{}^D \cong C^A_{LUMO}\, C^D_{LUMO}\, \beta_{AD} \cos(\Theta_{AD}) + \text{const} \tag{16}$$

Expressions 15 and 16 are valid only for the interactions with the ^{1}LE states mainly described by a configuration corresponding to an electron jump from HOMO to LUMO (e.g. ^1L_a states of the studied subunits). Higher UMO and lower OMO orbitals should be considered if the given interacting LE state is described using the configuration interaction (CI). The small values (0.153, 0.00) of the coefficients of the LUMO and LUMO + 1 orbitals at the carbazole nitrogen atom explain the absence of any significant intensity "borrowing" from the donor subunit. The corresponding effect originating from the acceptors is not operative because of relatively large energy gap between the acceptor LE and ^{1}CT states. The large value (0.503) of the LCAO coefficient of the HOMO orbital at the carbazole nitrogen atom agrees well with the dominant role of the interactions between the emitting ^{1}CT and the ground states.

The values of the appropriate LCAO coefficients of the donor LUMO (and higher UMO) orbitals and of the acceptor HOMO (and lower OMO) explain also (at least qualitatively) the effects observed in the phosphorescence spectra. For example, the red shift of the phosphorescence maxima can be explained by taking into accounts the stabilizing interaction between the lowest excited ^{3}LE and CT states. The appropriate values of the products $C^A_{HOMO}\, C^D_{HOMO}$ and $C^A_{LUMO}\, C^D_{LUMO}$ suggest that such interactions should be relatively weak for the locally excited triplets within the donor and stronger for the acceptor moieties (the respective energy gaps are similar). Moreover, the observed effects should be largest for the para isomers. Both predictions are really observed in the recorded phosphorescence spectra (cf. Figures 5 and 6), but further investigations of the nature of the lowest emissive triplet states are required for the more detailed discussion.

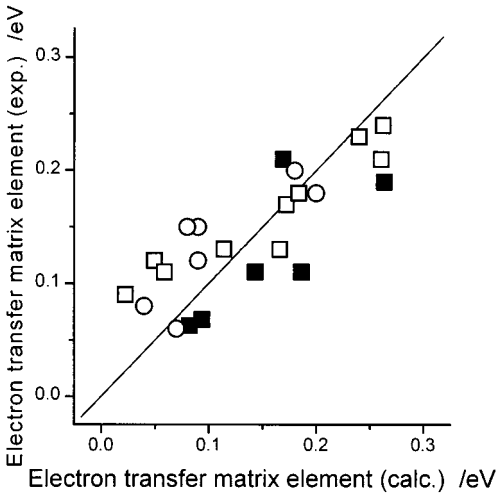

Figure 13. Correlation between the experimental and calculated (according to eq 13) values of the electronic matrix elements V_0 describing the electronic coupling between the excited charge transfer ^{1}CT state and the ground state S_0: (■) carbazol-9-yl derivatives of aromatic ketones, (□) carbazol-9-yl derivatives of aromatic nitriles,[13] and (○) 9-acridyl derivatives of aromatic amines.[25]

3.5. Competition between Radiative and Radiationless Transitions. As mentioned above, the nonradiative depopulation of the lowest excited ^{1}CT state of the studied compounds is most probably controlled by two competitive mechanisms: (i) the intersystem crossing (ISC) to the triplet manifold and (ii) a direct radiationless charge recombination (DICR) to the ground S_0 state in the singlet manifold. The efficiency of the radiationless depopulation path via the triplet manifold in various A−D systems should depend on the energy of the ^{3}LE states with respect to that of the CT state. To examine the latter process it should be recognized to what degree the nonradiative deactivation of the ^{1}CT state can be assigned to the DICR path. The decrease of the CT fluorescence intensity with the growing solvent polarity for all of the studied A−D derivatives suggests that the DICR channel is the dominant radiationless deactivation path in the polar media. To test this hypothesis, the experimental rate constants of the DICR (k_{nr} values in highly polar solvents such as DMF) can be compared with those calculated from the following relation[60]

$$k_{nr} = \frac{4\pi^2}{h} V_0^2 \sum_{j=0} \frac{e^{-s} S^j}{j!} \sqrt{\frac{1}{4\pi\lambda_o k_B T}} \exp\left[-\frac{(\Delta G_{CT} + \lambda_o + jh\nu_i)^2}{4\lambda_o k_B T} \right] \quad (17)$$

where the values of ΔG_{CT}, λ_o, $h\nu_i$, and S are derived from the band-shape analysis of the CT fluorescence spectra (eq 4) and those of the electronic coupling elements V_0 from the investigations of the radiative properties of the ^{1}CT states. The discrepancies between the experimental nonradiative rate constants k_{nr} and the values calculated from eq 17 for the studied A−D derivatives are smaller than 1 order of magnitude (cf. Table 4) which may be regarded as satisfactory (especially taking into account the number of the parameters going into calculations). The obtained results illustrate that, similarly to electron transfer in contact radical ion pairs,[6−11] the Marcus theory can be used for at least a semiquantitative description of the electron transfer rate constants also in the intramolecular donor−acceptor systems. Moreover, similarly as it was found previously[13] for carbazol-9-yl derivatives of aromatic nitriles, ISC processes can be neglected in the polar media.

TABLE 4: Comparison between Experimental (Eq 11) and Computed (Eq 17) k_{nr} Values (Data in *N,N*-Dimethylformamide Solutions)[a]

substance	V_0 (eV)	λ_i (eV)	$h\nu_i$ (eV)	λ_o (eV)	ΔG_{CT} (eV)	k_{nr}(exptl) (10^7 s^{-1})	k_{nr}(calcd) (10^7 s^{-1})
CPB	0.21	0.26	0.19	0.69	3.09	7.2	48
COB	0.11	0.28	0.20	0.38	2.81	9.0	15
CMB	0.063	0.30	0.19	0.60	2.95	4.6	26
CPA	0.19	0.27	0.20	0.63	3.16	7.0	21
COA	0.11	0.30	0.20	0.43	3.02	5.5	7.1
CMA	0.068	0.31	0.19	0.63	3.13	4.1	9.9

[a] The values of the outer (λ_o) and inner (λ_i) reorganization energies, the free energy gap ΔG_{CT}, and the vibrational quanta $h\nu_i$ as computed from CT emission band-shape analysis (eq 4). The electronic matrix elements V_0 calculated from the experimental electronic transition dipole moment (Table 1) according to eq 13 (with neglect of possible contribution from the locally excited states, see text).

According to the energy gap rule (i.e., the energy difference between ^{1}CT state and S_0 state) lowering of k_{nr} rate should follow the decrease of the solvent polarity. In the studied cases it is indeed observed in the moderately polar solvents (like EA or DME) with the maximal values of the fluorescence quantum yields. In nonpolar (HEX or MCH) or low polar media (BE) lack (or only traces) of the room temperature emission clearly indicates the opening of another nonradiative deactivation channel, most probably an ISC process. More detailed inspection in the results of the CT band-shape analysis (ΔG_{CT} values) and comparison of the computed ΔG_{CT} values with the energies of the locally excited triplet ^{3}LE states (of the donor and acceptor subunits) support the above explanation. The studied A−D molecules emit intense fluorescence if the energies of their emissive ^{1}CT states are equal or smaller than 3.10−3.25 and 2.95−3.10 eV for acetophenone and benzophenone derivatives, respectively. The corresponding energies for the lowest triplet states (0−0 transition in the parent acceptor phosphorescence spectra) are 3.20 and 3.00 eV. For the donor subunit (3,8-di-*tert*-butylcarbazole) the corresponding transition is localized at 3.05 eV. In nonpolar solvents the corresponding ΔG_{CT} values (extrapolated according to eq 5) are distinctly higher than the energies of the locally excited triplets and correspondingly the fast transition ^{1}CT → ^{3}LE may take place. Contrary to that, in the polar media ^{1}CT states are situated below the locally excited triplets and ISC processes do not occur. Solvents like IPE or EE (in which the room temperature fluorescence appears) seem to be a border case. The above conclusions are summarized in Figure 14 which presents the corresponding processes and energy level diagrams.

It becomes evident that the observed very fast ISC process in nonpolar solvents is connected with the $^3(n,\pi^*)$ nature of the lowest acceptor triplet and arises from the spin−orbit coupling effect caused by the oxygen atom from the carbonyl groups. In the case of benzophenone derivatives the lowest $^3(n,\pi^*)$ triplet state (localized within the acceptor subunit) is populated directly. In the case of acetophenone derivatives, however, the reaction mechanism is somewhat more complicated. The $^3(n,\pi^*)$ triplet state of the acceptor subunit seems to be an intermediate which undergoes the excitation energy transfer into the lower $^3(\pi,\pi^*)$ triplet state (localized within the donor subunit). Similarly as was observed in the cases of *N*-carbazolyl derivatives of aromatic nitriles,[13,27] the direct population of this lowest excited triplet state in the acetophenone derivatives is much slower. The mechanism as discussed above seems to be the most probable from the kinetic point of view, but detailed transient absorption

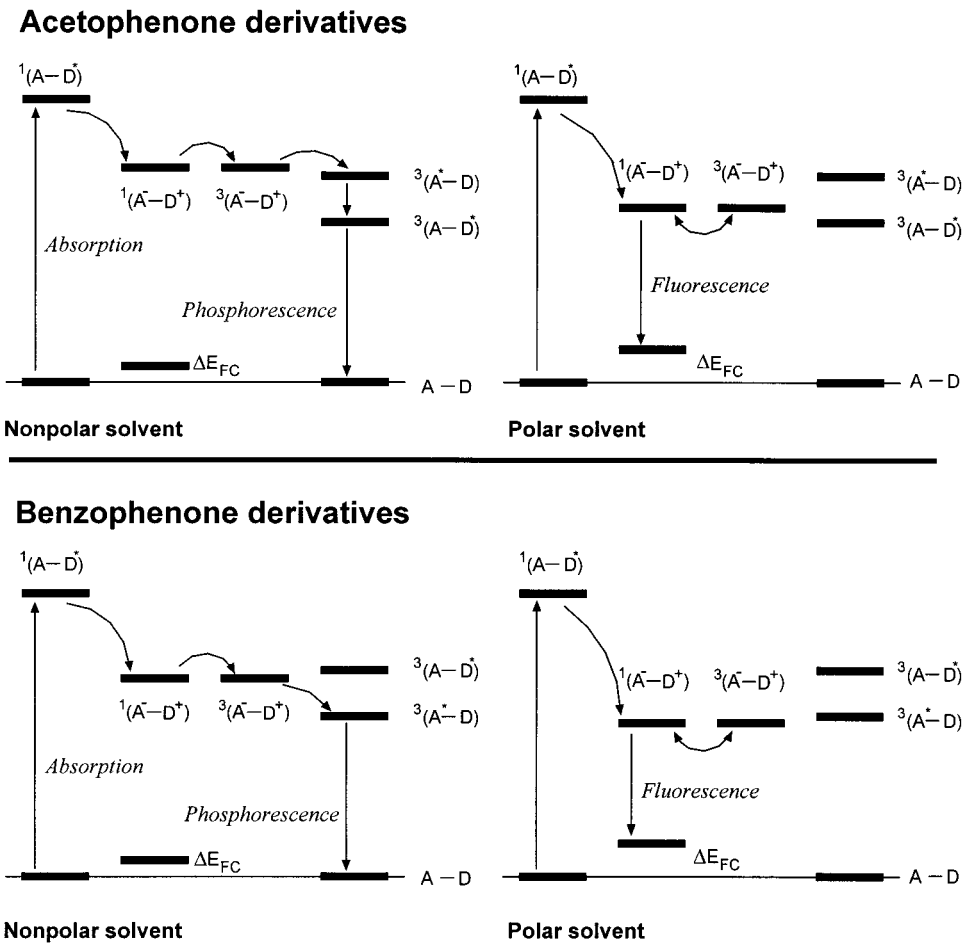

Figure 14. Energy levels diagrams for carbazol-9-yl derivatives of acetophenone (top) and benzophenone (bottom) in nonpolar and polar solvents, respectively.

investigations are necessary for more advanced discussion and for the confirmation of the solvent polarity induced changes in the reaction mechanism. The increase of the solvent polarity (and, correspondingly, the decrease of the ^{1,3}CT states energy) not only induces the changes in the competition between two nonradiative deactivation channels but also should lead to the different electronic structure of the lowest triplet state in the given A−D molecule. It arises from the switching from the stabilizing (nonpolar media) to the destabilizing (polar media) interactions between the CT state and the locally excited ^{3}LE triplet state (in the acceptor or donor subunits). In nonpolar media the electronic interactions are stabilizing because the ^{1,3}CT states are energetically located above of the locally excited triplets. It is indeed observed in the phosphorescence spectra. On the contrary, in higly polar solvents the ^{1,3}CT states for the studied A−D systems seem to be localized below the locally excited triplets. The wave function of the lowest triplet state in the studied A−D molecules should have a considerable amount of the CT character, similarly as it was reported for the carbazol-9-yl derivatives of dicyanobenzenes.[27]

4. Concluding Remarks

Radiative and radiationless charge recombination processes exemplified respectively by the CT fluorescence and direct radiationless charge recombination to the ground state in the singlet manifold have been studied in a series of N-bonded donor−acceptor derivatives of 3,6-di-*tert*-butylcarbazole containing acetophenone and benzophenone as an electron acceptor. The investigations of the solvent effects on the spectral position and band shape of the CT absorption and emission allowed to estimate the energy levels for the A−D molecules studied. A very good agreement between two independent estimations of the energy levels of the ^{1}CT states based on the two independent ways, i.e., electrochemical and the photophysical, is observed.

The analysis of the CT fluorescence profile leads to the quantities relevant for the electron transfer in the Marcus inverted region. The obtained values suggest that the studied A−D derivatives do not undergo any significant low-frequency intramolecular nuclear motions (e.g., rotations) upon excitation. The twist angle between the donor and acceptor moieties in the emitting ^{1}CT state seems to be similar to that in the ground state. This hypothesis agrees well with the values of the fluorescence rate constants (k_f) and the corresponding transition dipole moments (M). The probabilities of the radiative electron transfer exemplified by the CT fluorescence can be correlated with the magnitude of the LCAO coefficient of the acceptor LUMO orbital at the position of the donor−acceptor bond. The large value of the LCAO coefficient of the HOMO orbital at the carbazole nitrogen atom and the small one of the corresponding coefficient of the LUMO orbital are responsible for the dominant role of the electronic interactions between the emitting ^{1}CT state and the ground state. Moreover, the obtained results illustrate again that, similarly to electron transfer in contact radical ion pairs, the Marcus theory can be used for the quantitative description of the radiationless electron transfer rate constants also in the intramolecular donor−acceptor systems with the same set of the parameters going into theory. Of course it is possible only when ISC processes can be neglected.

The presented results support a possibility to predict the properties and photophysical behavior of the A−D compounds from the properties of the donor and acceptor subunits forming the A−D molecule. It may be done taking into account the relative energies of the locally excited states (within the A and D subunits) and the redox potentials of the donor and acceptor groups as well as from the interaction between them. The respective values of the electronic matrix elements describing the electronic coupling between the lowest excited charge transfer state ^{1}CT and the ground state S_0 or the locally excited states may be predicted from the appropriate LCAO coefficients on the atoms forming the donor−acceptor bond. This work together with the previously reported results[13,24,25,27,61] indicates that such predictions lead to the quantitative description of the properties of the intramolecular charge-transfer states. It may be important from the practical point of view because the proposed approach allows the discussion of the mutual orientation of the donor and acceptor subunits. Most probably, currently investigated A−D aromatic systems allow us to test this simple model both for the fluorescent ^{1}CT states and the lowest ^{3}CT triplet states. Moreover, the described intramolecular donor−acceptor compounds have an appropriate sequence of excited states (in polar solvents) to design new electrochemiluminescent systems[62,63] with extremely high efficiencies. Work in this direction is being continued.

Acknowledgment. This work was sponsored by grant 3T09A06214 from the Committee of Scientific Research. Special thanks are also due to the Foundation for Polish Science for the donation of the FS 900 CDT and FL 900 CDT fluorometers from Edinburgh Analytical Instruments. Technical assistance from Mrs. A. Zielińska and Mrs. B. Osińska is deeply appreciated.

References and Notes

(1) *Photoinduced electron transfer (Parts A−D)*; Fox, M. A., Chanon, M., Eds.; Elsevier: Amsterdam, 1988.

(2) Kavarnos, G. J. *Fundamentals of Photoinduced Electron Transfer*; VCH: New York, 1994.

(3) (a) Ulstrup, J.; Jortner, J. *J. Chem. Phys.* **1975**, *63*, 4358. (b) Marcus, R. A.; Sutin, N. *Biochim. Biophys. Acta* **1985**, *811*, 265.

(4) (a) Hush, N. S. *Prog. Inorg. Chem.* **1967**, *8*, 391. (b) Hush, N. S. *Electrochim. Acta* **1968**, *13*, 1005. (c) Hush, N. S. *Coord. Chem. Rev.* **1985**, *64*, 135.

(5) Marcus, R. A. *J. Phys. Chem.* **1989**, *93*, 3078 and references cited therein.

(6) Gould, I. R.; Farid, S. *J. Photochem. Photobiol. A: Chem.* **1992**, *65*, 133.

(7) Gould, I. R.; Young, R. H.; Moody, R. E.; Farid, S. *J. Phys. Chem.* **1991**, *95*, 2068.

(8) Gould, I. R.; Noukakis, D.; Gomez-Jahn, L.; Young, R. H.; Goodman, J. L.; Farid, S. *Chem. Phys.* **1993**, *176*, 439.

(9) Gould, I. R.; Noukakis, D.; Gomez-Jahn, L.; Goodman, J. L.; Farid, S. *J. Am. Chem. Soc.* **1993**, *115*, 4405.

(10) Gould, I. R.; Young, R. H.; Mueller, L. J.; Farid, S. *J. Am. Chem. Soc.* **1994**, *116*, 8176.

(11) Gould, I. R.; Young, R. H.; Mueller, L. J.; Albrecht, A. C.; Farid, S. *J. Am. Chem. Soc.* **1994**, *116*, 8188.

(12) Cortes, J.; Heitele, H.; Jortner, J. *J. Phys. Chem.* **1994**, *98*, 2527 and references cited therein.

(13) Kapturkiewicz, A.; Herbich, J.; Karpiuk, J.; Nowacki, J. *J. Phys. Chem. A* **1997**, *101*, 2332.

(14) (a) Oevering, H. Ph.D. Dissertation, University of Amsterdam, Amsterdam, The Netherlands, 1988. (b) Oevering, H.; Verhoeven, J. W.; Paddon-Row, M. N.; Warman, M. J. *Tetrahedron* **1989**, *45*, 4751.

(15) Oliver, A. M.; Paddon-Row, M. N.; Kroon, J.; Verhoeven, J. W. *Chem. Phys. Lett.* **1992**, *191*, 371.

(16) Mulliken, R. S. *J. Am. Chem. Soc.* **1952**, *74*, 811.

(17) Beratan, D.; Hopfield, J. J. *J. Am. Chem. Soc.* **1984**, *106*, 1584.

(18) (a) Mataga, N.; Murata, Y. *J. Am. Chem. Soc.* **1969**, *91*, 3144. (b) Mataga, N. In *The Exciplex*; Gordon, M., Ware, W. R., Eds.; Academic Press: New York, 1975. (c) Masaki, S.; Okada, T.; Mataga, N.; Sakata, Y.; Misumi, S. *Bull. Chem. Soc. Jpn.* **1976**, *49*, 1277.

(19) (a) Pasman, P. Ph.D. Dissertation, University of Amsterdam, Amsterdam, The Netherlands, 1980. (b) Pasman, P.; Rob, F.; Verhoeven, J. W. *J. Am. Chem. Soc.* **1982**, *104*, 5127.

(20) Bixon, M.; Jortner, J.; Verhoeven, J. W. *J. Am. Chem. Soc.* **1994**, *116*, 7349 and references cited therein.

(21) Verhoeven, J. W.; Scherer, T.; Wegewijs, B.; Hermant, R. M.; Jortner, J.; Bixon, M.; Depaemelaere, S.; De Schryver, F. C. *Recl. Trav. Chim. Pays-Bas* **1995**, *114*, 443.

(22) Herbich, J.; Kapturkiewicz, A. *Chem. Phys.* **1991**, *158*, 143.

(23) Herbich, J.; Kapturkiewicz, A. *Chem. Phys.* **1993**, *170*, 221.

(24) Herbich, J.; Kapturkiewicz, A. *Chem. Phys. Lett.* **1997**, *273*, 8.

(25) Herbich, J.; Kapturkiewicz, A. *J. Am. Chem. Soc.* **1998**, *120*, 1014.

(26) Dogonadze, R. R.; Kuznetsov, A. M.; Marsagishvili, T. A. *Electrochim. Acta* **1980**, *25*, 1.

(27) Herbich, J.; Kapturkiewicz, A.; Nowacki, J. *Chem. Phys. Lett.* **1996**, *262*, 633.

(28) Neugebauer, F. A.; Fischer, H. *Chem. Ber.* **1972**, *105*, 2686.

(29) Khan, M. A.; Polya, J. B. *J. Chem. Soc. (C)* **1970**, 5.

(30) Reichardt, C. *Solvent Effects in Organic Chemistry*; VCH: Weinheim, New York, 1979.

(31) Velapoldi, R. A. *Natl. But. Std. 378, Proc. Conf. NBS, Gaithersburg* **1972**, 231.

(32) Kapturkiewicz, A.; Grabowski, Z. R.; Jasny, J. *J. Electroanal. Chem.* **1990**, *279*, 55.

(33) Kapturkiewicz, A. *J. Electroanal. Chem.* **1993**, *348*, 283.

(34) Bigelow, R. W.; Johnson, G. E. *J. Phys. Chem.* **1977**, *66*, 4861.

(35) Gudipati, M. S.; Daverkausen, J.; Maus, M.; Hohlneicher, G. *Chem. Phys.* **1994**, *186*, 289, and the literature cited therein.

(36) *DMS UV Atlas of Organic Compounds*; VCH and Butterworths: Weinheim and London, 1966.

(37) *The Sadtler Handbook of Ultraviolet Spectra*; Sadtler Research Laboratory: Philadelphia, PA, 1979.

(38) McGlynn, S. P.; Azumi, T.; Kinoshita, M. *Molecular spectroscopy of the triplet state*; Prentice Hall: Englewood Cliffs, NJ, 1969, and references therein.

(39) Murov, S. L.; Carmichael, I.; Hug, G. L. *Handbook of Photochemistry*; Marcel Dekker: New York, 1993.

(40) Böttcher, C. J. F. In *Theory of electric polarization*; Van Belle, O. C., Bordewijk, P., Rip, A., Eds.; Elsevier: Amsterdam, 1973; Vol. 1.

(41) Lippert, E. *Z. Naturforsch.* **1955**, *10a*, 541.

(42) Mataga, N.; Kaifu, Y.; Koizumi, M. *Bull. Chem. Soc. Jpn.* **1955**, *28*, 690.

(43) Liptay, W. In *Excited States*; Lim, E. C., Ed.; Academic Press: New York, 1974; p 129.

(44) McRae, E. G. *J. Phys. Chem.* **1957**, *61*, 562.

(45) Onsager, L. *J. Am. Chem. Soc.* **1936**, *58*, 1486.

(46) Ambroese, J. F.; Carpentier, L. L; Nelson, R. F. *J. Electrochem. Soc.* **1975**, *122*, 876.

(47) Evans, D. H. In *Encyclopedia of the Electrochemistry of the Elements*; Bard, A. J., Lunds, H., Eds.; Marcel Dekker: New York, 1978; Vol. 12, p 3.

(48) Bader, J. S.; Berne, B. J. *J. Chem. Phys.* **1996**, *104*, 1293.

(49) Weller, A. *Z. Phys. Chem. (Münich)* **1982**, *133*, 93.

(50) Grabowski, Z. R.; Dobkowski, J. *Pure Appl. Chem.* **1983**, *55*, 245.

(51) Auty, A. R.; Jones, A. C.; Phillips, D. *Chem. Phys.* **1986**, *103*, 163.

(52) Birks, J. B. In *Photophysics of Aromatic Molecules*; Wiley: New York, 1978; p 48.

(53) Mulliken, R. S. *J. Am. Chem. Soc.* **1952**, *74*, 811.

(54) Murrell, J. N. *J. Am. Chem. Soc.* **1959**, *81*, 5037.

(55) McConnell, H. M. *J. Chem. Phys.* **1956**, *24*, 632, 764.

(56) Klöpffer, W.; Kaufmann, G.; Naudorf, G. *Z. Naturforsch.* **1971**, *26a*, 897.

(57) Steinberg, N.; Fraenkel, G. K. *J. Chem. Phys.* **1964**, *40*, 723.

(58) Rieger, P. H.; Fraenkel, G. K. *J. Chem. Phys.* **1962**, *37*, 2811.

(59) Avendaño, C.; Espada, M.; Ocaño, B.; Garcia-Granda, S.; del Rosario Diaz, M.; Tejerina, B.; Gómez-Beltrán, F.; Martinez, A.; Elguero, J. *J. Chem. Soc., Perkin Trans. 2* **1993**, 1547.

(60) Efrima, S.; Bixon, M. *Chem. Phys. Lett.* **1974**, *25*, 341.

(61) Borowicz, P.; Herbich, J.; Kapturkiewicz, A.; Nowacki, J. *Chem. Phys.* **1999**, *244*, 251.

(62) Kapturkiewicz, A.; Herbich, J.; Nowacki, J. *Chem. Phys. Lett.* **1997**, *275*, 355.

(63) Kapturkiewicz, A. In *Advances in Electrochemical Sciences and Engineering*; Alkire, R., Gerischer, H., Kolb, D. M., Tobias, C. W., Eds.; Wiley-VCH: Weinheim, Germany 1997; Vol. 5, p 1.